

Expression Snippet Transformer for Robust Video-based Facial Expression Recognition

Yuanyuan Liu¹, Wenbin Wang¹, Chuanxu Feng¹, Haoyu Zhang¹, Zhe Chen^{*2}, and Yibing Zhan³

¹China University of Geosciences (Wuhan)

¹{liuyy, wangwenbin, fcxfcx, zhanghaoyu}@cug.edu.cn

²The University of Sydney

²zhe.chen1@sydney.edu.au

³Jingdong

³zhanyibing@jd.com

September 20, 2021

Abstract

The recent success of Transformer has provided a new direction to various visual understanding tasks, including video-based facial expression recognition (FER). By modeling visual relations effectively, Transformer has shown its power for describing complicated patterns. However, Transformer still performs unsatisfactorily to notice subtle facial expression movements, because the expression movements of many videos can be too small to extract meaningful spatial-temporal relations and achieve robust performance. To this end, we propose to decompose each video into a series of expression snippets, each of which contains a small number of facial movements, and attempt to augment the Transformer’s ability for modeling intra-snippet and inter-snippet visual relations, respectively, obtaining the Expression snippet Transformer (EST). In particular, for intra-snippet modeling, we devise an attention-augmented snippet feature extractor (AA-SFE) to enhance the encoding of subtle facial movements of each snippet by gradually attending to more salient information. In addition, for inter-snippet modeling, we introduce a shuffled snippet order prediction (SSOP) head and a corresponding loss to im-

prove the modeling of subtle motion changes across subsequent snippets by training the Transformer to identify shuffled snippet orders. Extensive experiments on four challenging datasets (*i.e.*, BU-3DFE, MMI, AFEW, and DFEW) demonstrate that our EST is superior to other CNN-based methods, obtaining state-of-the-art performance. Our code and the trained model are available at <https://anonymous.4open.science/r/ATSE-C58B>

1 Introduction

Video-based Facial Expression Recognition (FER) is important for understanding human emotions and behaviors in videos, benefiting various applications such as digital entertainment, customer service, driver monitoring, emotion robots, etc. [51, 39, 45, 22]. FER aims to classify a video into one of several basic emotions, including happiness, anger, disgust, fear, sadness, neutral, and surprise. The task of FER is difficult due to several challenges, namely, long-range spatial-temporal representation, excessive noises from irrelevant frames, and especially, inherently *small* and *subtle* facial movements in FER videos.

To tackle the issues of FER, existing methods com-

^{*}Corresponding author

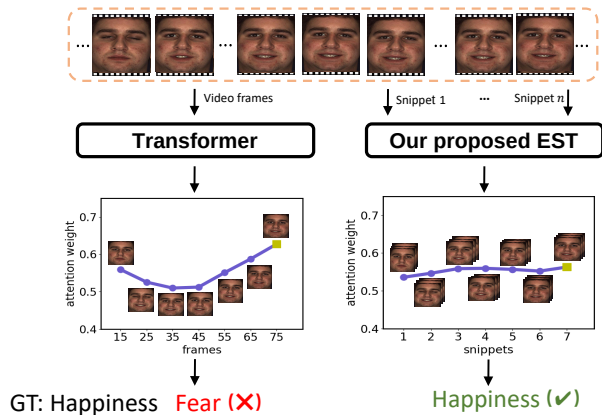


Figure 1: Comparison between a vanilla Transformer and the proposed expression snippet Transformer (EST) for modeling subtle facial expression movements in facial expression recognition (FER). The vanilla Transformer (left) tends to focus only on the frame with peak expression patterns and can be easily affected by noises such as other non-expression changes, thus obtaining sub-optimal results. By decomposing videos into snippets, the EST (right) improves the modeling of intra-snippet and inter-snippet subtle facial changes, respectively, and can achieve more robust FER.

monly apply convolutional neural networks (CNNs) or long-short term memory (LSTM). However, most of the existing FER methods usually model spatial-temporal visual information without involving effective visual relation reasoning mechanisms. For example, many methods [14, 44, 23, 46, 19] only use static frames selected from the manually defined peak (apex) frames, neglecting the intrinsic relationships between visual cues of adjacent frames. Sequence-based methods [10, 11, 3, 5] attempt to capture motion cues by encoding spatial-temporal information within their models. However, Sequence-based methods still perform weakly in describing subtle expression movements in FER videos. Besides, they usually require overwhelmingly large model capacities to help model subtle facial changes [24].

The recent successful Transformer approaches [8, 28, 38] in computer vision has allowed us to take advantage of its powerful relation reasoning ability for understanding FER videos. In general, the Transformer [42] has been shown to be particularly effective for translating an

input sequence to a target sequence by modeling the relations between features. Accordingly, for video-based FER, we suggest that the Transformer has a great potential of describing subtle expression movements more robustly. However, despite the potential advantages, it is non-trivial to directly apply the vanilla Transformer on the FER videos, considering the subtle facial expression movements of videos that are difficult to be noticed by vanilla Transformer. For example, as shown in Fig. 1, the per-frame visual information, raw pixels on each frame, may contain noises such as other non-expression changes (head poses, speaking, and so on) that can easily affect the recognition performance of the Transformer. Furthermore, the subtle expression movements would make the Transformer only focus on the visual cues from frames with peak expression changes and neglect plenty of beneficial spatial-temporal information from other periods of videos. This limits the potential of Transformer to encode the motion information of the entire video comprehensively and achieve more robust expression recognition.

To tackle the above problems for applying Transformer on FER videos, we first propose to decompose the facial movements of the entire video into a series of small expression snippets. Each expression snippet is a video clip with a few adjacent frames of the input video covering a limited amount of expression changes. Then, by employing the Transformer over the snippets, we can augment the modeling of intra-snippet and inter-snippet expression movements, respectively. In particular, we introduce a novel attention-augmented snippet feature extractor (AA-SFE) to improve the modeling of intra-snippet visual changes for the Transformer. In the AA-SFE, we apply a deep convolutional neural network (DCNN) to extract per-frame visual features and develop a novel hierarchical attention-augmentation architecture to obtain the representation of facial movements within each snippet. The snippet representations generated with the AA-SFE are subsequently fed into the encoder-decoder structure of the Transformer to perform recognition based on snippet-level relations. Meanwhile, we devise a shuffled snippet order prediction (SSOP) head with a corresponding loss for the Transformer to improve the modeling of inter-snippet visual changes. By using SSOP, the Transformer can encode the information from all snippets more comprehensively, thereby delivering a more robust expression movement representation of the entire video. Overall, we

briefly name our proposed method as expression snippet Transformer (EST).

To sum up, the major contributions of this paper are summarized as follows:

- We propose the expression snippet Transformer (EST) to achieve accurate video-based facial expression recognition (FER). To the best of our knowledge, our approach is the first effective snippet-based Transformer method for video-based FER.
- To enhance the Transformer’s ability to model intra-snippet and inter-snippet expression movements, we propose the attention-augmented snippet feature extractor (AA-SFE) and the shuffled snippet order prediction (SSOP), respectively. Both techniques effectively tackle the problems of Transformer-based FER and substantially improves the recognition performance.
- Evaluations on four challenging video facial expression datasets, *i.e.*, BU-3DFE, MMI, AFEW, and DFEW, demonstrate the superiority of our proposed EST over existing popular methods. State-of-the-art performance can be achieved with EST on the evaluated datasets.

2 Related Work

Frame-based methods The frame-based methods can be divided into two groups: frame aggregation methods that strategically fuse deep features learned from static-based FER networks [32, 20] and peak frame extraction methods that focus on recognizing the peak high-intensity expression frame [52, 49]. Meng *et al.* [32] proposed frame attention networks to adaptively aggregate frame features in an end-to-end framework and achieved an accuracy of 51.18% on the AFEW 8.0 dataset. Zhao *et al.* [52] proposed a peak-piloted deep network (PPDN) for intensity-invariant expression recognition. Moreover, Yu *et al.* [49] proposed a deeper cascaded peak-piloted network (DCPN) that enhances the discriminative ability of features in a cascade fine-tuning manner. The PPDN and DCPN respectively achieved the best accuracies of 99.3% and 99.9% on the CK+ dataset [29]. However, these methods depend only on static frames and lack powerful mod-

eling of the spatial-temporal relationships of expressions in the video.

Dynamic sequence-based methods In order to explore the spatial-temporal representation of expressions, dynamic sequence-based methods take a video sequence as a single input and utilize both textural information and temporal dependencies in the sequence for more robust expression recognition [17, 18, 19, 43, 24]. Recently, the Long Short-Term Memory (LSTM) and C3D are two widely-used spatial-temporal methods. Vielzeuf *et al.* [43] firstly used pre-trained VGG-Face to extract spatial features, then utilized LSTM layers to encode temporal dependencies in a sequence. Kim *et al.* [18] proposed a new spatio-temporal feature representation learning for FER by integrating C3D and LSTM networks, which is robust to expression intensity variations. Although the C3D networks can capture the spatial-temporal change of an expression, the C3D networks introduce expensive space- and computational complexity to learn subtle expression movements more effectively.

Transformer Transformer was introduced by Vaswani *et al.* [42] as a new attention-based building block for machine translation. Transformer included self-attention layers to scan through each token in a sequence and learn the tokens’ relationships by aggregating information from the whole sequence, replacing RNNs in many tasks, such as natural language processing (NLP), speech processing, and computer vision [8, 28, 38, 36, 34, 6]. Recently, Nicolas *et al.* expanded the basic Transformer architecture to the field of object detection and proposed the DETR algorithm [4]. Girdhar *et al.* proposed an action Transformer to aggregate features from the spatial-temporal contexts around persons for action recognition in a video [33]. Transformer has been successfully applied for computer vision tasks, such as objection detection and action recognition. However, applying the vanilla Transformer to capture subtle expression movements in an untrimmed video is still challenging due to the noises and the limited motion variations within input frames.

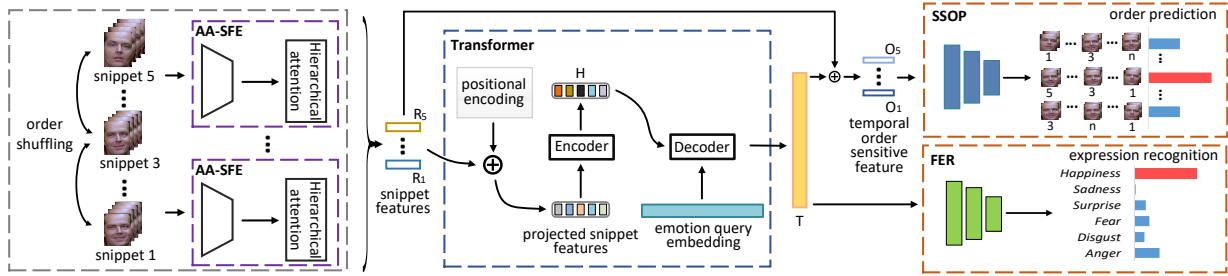


Figure 2: The training pipeline of the EST for video-based FER. Using expression snippets, we apply the AA-SFE and SSOP head to improve Transformer’s ability to model intra-/inter-snippet expression movements and relevance, thus achieving robust FER.

3 Expression Snippet Transformer

3.1 EST architecture

The overall EST architecture is illustrated in Fig. 2. Firstly, we collect expression snippets from the input video. For each snippet, we apply the AA-SFE to extract per-snippet features. Then, we employ a Transformer with a SSOP head to achieve robust expression understanding. In the following sections, we will subsequently explain the Expression snippets, Transformer, AA-SFE, and SSOP.

Expression snippets We decompose the input video into a series of snippets to augment the Transformer’s ability to model subtle visual changes within each snippet and across different snippets, respectively. Formally, given an input FER video \mathcal{C} , we decompose it into a series of smaller sub-videos: $\mathcal{C} = \{C_1, C_2, \dots, C_n\}$, where C_i represents the i -th sub-video and n is the total number of sub-videos. Each sub-video C_i refers to an expression snippet that contains several adjacent frames of the video. All the snippets have the same length, and they follow consecutive orders along time.

Transformer Architecture We first extract snippet features with AA-SFE, which will be discussed later. With the snippet features, a Transformer is applied here to model the expression movements across snippets and discover a more robust emotion representation for FER. We follow the typical Transformer formulation and apply a multi-head attention-based encoder-decoder pipeline for the processing. In general, the multi-head attention estimates the correlation between a *query* tensor and a *key*

tensor and then aggregates a *value* tensor according to correlation results to obtain an attended output. For more details of the Transformer, please refer to [42].

In our approach, we employ the encoder to encode snippet features and then use the decoder to translate the encoded features into a more robust expression representation. Let $R_i \in \mathbb{R}^d$ denote the extracted snippet feature of C_i with a size of d , and $\mathcal{R} = \{R_1, R_2, \dots, R_n\}$. We feed \mathcal{R} to the encoder of the Transformer in EST. In the encoder, for each head of the multi-head attention, we perform linear projections on a snippet feature R_i to obtain the corresponding query vector q_i , key vector k_i , and value vector v_i , respectively. All the q_i, k_i, v_i are vectors of size d as well.

Then, we stack different snippets’ query vectors, key vectors, and value vectors to obtain a query tensor Q , a key tensor K , and a value tensor V , respectively. $Q, K, V \in \mathbb{R}^{n \times d}$. Afterward, we perform self-attention across the snippets based on the obtained Q, K , and V . In addition, we apply a snippet positional encoding to describe the positions of snippets within a video, following the sine and cosine positional encoding [42]. The output of the encoder is the encoded snippet features $H \in \mathbb{R}^{n \times d}$:

$$H = A(Q, K, V) = \text{softmax}\left(\frac{QK^T}{\sqrt{d}}\right)V, \quad (1)$$

where $A(\cdot)$ represents the self-attention. In this study, we employ 3 encoder layers, each with 4 attention heads.

After encoding snippet features with self-attention, the decoder phase then applies cross-attention to decode the encoded features H into an emotion representation T and $T \in \mathbb{R}^d$. We introduce an *emotion query embedding* for

the decoder to represent the query tensor of the multi-head attention. The emotion query embedding shares the same dimension with T . We use the encoded feature H to represent both key and value tensors in the decoder. In practice, we stack 3 decoder layers, each with 4 attention heads, to progressively refine the decoding results.

After the encoder-decoder processing, we make the Transformer provide two outputs, forming two prediction heads. The first head, built upon a 3-layer perception network, is the expression recognition prediction, classifying the T into different expression types. The second head is the SSOP, which estimates the correct snippet order since snippets are shuffled. We will discuss the details of SSOP later.

3.2 Attention-augmented Snippet Feature Extraction

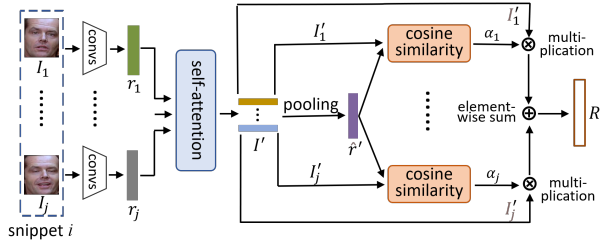


Figure 3: The detailed architecture of the AA-SFE.

Directly applying the Transformer on raw frames can be sub-optimal due to visual noises within pixels, making it difficult to obtain robust expression representation. Using snippets, we boost the Transformer to better model intra-snippet expression movements by introducing a novel attention-augmented snippet feature extractor (AA-SFE). AA-SFE improves the encoding of spatial-temporal information across frames within a snippet.

Fig. 3 shows the structure of an AA-SFE. In particular, with the help of normal DCNNs, such as a pre-trained ResNet-18, the AA-SFE applies a *hierarchical attention augmentation* for modeling intra-snippet information. The hierarchical attention aims to gradually extract a more representative feature of a snippet, progressively filtering out less meaningful non-expression information to reduce the negative impacts of noises within per-frame features. We mainly apply the attention from *two-level*

hierarchy to model subtle visual changes. The first level extracts frame-level attention, and the second focuses on extracting snippet-level global attention.

For the *first-level* hierarchy, we investigate frame-level relation to obtaining attention. Similar to the Transformer, we apply self-attention here for relation modeling. Mathematically, we use $r_{j,i}$ to represent the feature vector of the j -th frame in the i -th snippet. We extract the global average pooling output of a DCNN as the per-frame feature: $r_{j,i} \in \mathbb{R}^d$. Suppose each snippet has J frames. By stacking all the features $r_{j,i}$ from the i -th snippet, we obtain the tensor $I_i \in \mathbb{R}^{J \times d}$. Since we only consider frames of a single snippet at this stage, we drop the symbol i here for simplicity, *i.e.*, $I = I_i$, $r_j = r_{j,i}$ in this part. Using linear projections, we transform I into three tensors: query tensor I_Q , key tensor I_K , and value tensor I_V . Then, we apply self-attention described in Eq.1 on I_Q, I_K, I_V to obtain the attended feature $I' \in \mathbb{R}^{J \times d}$.

In the *second-level* hierarchy, we introduce the snippet-level global information to further refine representations of snippets. Firstly, we summarize the I' into a unified general feature vector. Then, we estimate the relations between the general feature and per-frame features. The obtained relations are later used to re-weight per-frame features for refinement. Lastly, the refined features are reduced to a single representation to describe the whole snippet. More specifically, we denote the symbol \hat{r}' as the general feature vector of I' , with a size of d . It is obtained by performing max pooling on I' across frames. Then, we estimate the relation between \hat{r}' and per-frame features using cosine similarity. We denote r'_j as the feature in I' correspond to the j -th frame. We compute cosine similarity α_j between \hat{r}' and each r'_j :

$$\alpha_j = \cos(r'_j, \hat{r}') = \frac{r'_j \cdot \hat{r}'}{\|r'_j\| \cdot \|\hat{r}'\|}, \quad (2)$$

where $\|\cdot\|$ means Euclidean norm. With the relation estimated by α_j , we can identify which frame contains more deviated information that could be more likely to contain noise with non-expression. Thus, we have the summarized snippet feature by re-weighting and aggregating per-frame features based on:

$$R_i = \frac{\sum_j \alpha_j \cdot r'_j}{\sum_j \alpha_j}. \quad (3)$$

To sum up, the self-attention of AA-SFE first provides powerful relation modeling to facilitate the encoding of frame-level spatial-temporal information. Then, we introduce the second hierarchy with cosine similarity-based attention modeling to consider the global motion information of a snippet to help further resist noises existing in per frame. According to Eq. 2 ~ 3, the attention can identify the more useful intra-snippet visual change information and facilitate the computation of a more focused snippet feature $R_i \in \mathbb{R}^d$. We experimentally prove that the AA-SFE delivers better snippet features comparing to a normal self-attention-based Transformer.

3.3 Shuffled Snippet Order Prediction

With the snippet features \mathcal{R} and the Transformer, we can estimate expressions of videos. However, we observe that the Transformer usually focuses only on the snippet with peak expression changes and neglects the rest parts of a video. This situation happens because the cross-attention modeling mechanism of Transformer probably easily overlooks the slight motion changes across subsequent snippets. In practice, the Transformer usually fails to deliver the comprehensive inter-snippet relation modeling for all the snippets and thus can be easily distracted by noisy information in the peak snippet. To make the Transformer model expression motions more comprehensively and avoid the negligence of subtle visual changes from off-peak snippets, we further introduce a shuffled snippet order prediction (SSOP) head with corresponding loss to assist training the EST. The algorithm of the SSOP is shown in Algorithm 1.

Algorithm 1 The Pseudo Code of the SSOP.

Input: FER video \mathcal{C} ; Permutated order S

Output: Predicted permuted order probability $p(S|O)$

- 1: $\{C_1, \dots, C_n\} \leftarrow \mathcal{C}$
 - 2: Shuffle the snippet order according to the S
 - 3: Collect features: $O_i = R_i + T$
 - 4: Concat features: $O = \text{Concat}([O_1, \dots, O_n])$
 - 5: Predict the snippet order probability $p(S|O)$
 - 6: Update SSOP head and emotion information T by Eq. 6
-

To train the Transformer with SSOP, we mainly shuffle the snippets and make the Transformer predict this shuffled snippet order. For example, if we have 7 snippets, a shuffled order can be like $S = (3, 2, 7, 1, 4, 6, 5)$. In practice, we generate 10 different types of different shuffled orders. Then, among all the generated orders, we sample one order and re-arrange the snippets accordingly. The snippets with a shuffled order are later sent to the EST. After extracting the emotion information T , we fuse the T with the $\mathcal{R} \in \mathbb{R}^{7 \times d}$ to obtain the features used for predicting shuffled orders. We name this type of feature as temporal order sensitive feature $O \in \mathbb{R}^{7 \times d}$. The computation of O can be found in Algorithm 1. We further apply three fully connected layers on the O to define the SSOP head, predicting the current permuted shuffling order. The prediction is obtained according to a classification output. Therefore, training the Transformer with the SSOP involves maximizing a posterior probability (MAP) estimate, where the related conditional probability density function is:

$$p(S|C_1, C_2, \dots, C_n) = p(S|O_1, \dots, O_n) \prod_{i=1}^n p(O_i|C_i), \quad (4)$$

where O_i is the feature vector in O for the i -th snippet. C_i represents i -th snippet.

In practice, without SSOP, although we have positional encoding in the Transformer, the snippet order and motion information from off-peak snippets is usually not well encoded due to very subtle facial changes. Alternatively, training the Transformer to identify shuffled snippet orders with SSOP can help ensure that information from every snippet is properly attended. As a result, the Transformer could become more sensitive to inter-snippet visual changes and more comprehensive to describe expression changes of the entire video. Besides, the SSOP also enriches the number of expression change patterns for training without requiring additional manual annotation.

3.4 Optimization Objectives

For training, the EST has two objectives. The first one is a FER classification loss L_{cls} , and the second one is a shuffled snippet order prediction loss L_S . We use the cross-entropy loss for optimization. Mathematically, the

FER loss L_{cls} can be written as:

$$L_{cls} = - \sum_c Y_c \cdot \log[\hat{Y}_c] + (1 - Y_c) \cdot \log[1 - \hat{Y}_c], \quad (5)$$

where Y_c denotes the facial expression label for each video, c indexes a training video, and \hat{Y}_c denotes the probabilities of facial expressions predicted by the EST.

To identity shuffled snippet order, we introduce the loss function L_S for SSOP based on:

$$L_S = - \sum_c S_c \cdot \log[\hat{S}_c] + (1 - S_c) \cdot \log[1 - \hat{S}_c], \quad (6)$$

where \hat{S}_c denotes the permutation type of the shuffled order predicted by the EST, and S_c is the ground truth one-vs-all label indicating the correct permutation type.

4 Experimental Results

4.1 Datasets

To evaluate our approach, four face expression datasets were used: BU-3DFE dataset [48], MMI dataset [41], AFEW8.0 dataset [9], and DFEW dataset [16].

BU-3DFE [48]: 3D facial expressions annotated with 6 emotion labels, *i.e.*, anger, disgust, happiness, fear, sadness, and surprise. BU-3DFE contains 606 3D facial expression sequences captured from 101 subjects. Each expression sequence contains nearly 100 frames.

MMI [41]: A total of 205 expression sequences were collected from 30 subjects. The expression sequences were recorded at a temporal resolution of 24 fps. Each expression sequence of the dataset was labeled with one of the six basic expression classes (*i.e.*, anger, disgust, fear, happiness, sadness, and surprise).

AFEW [9]: The AFEW serves as an evaluation platform for the annual EmotiW since 2013. Seven emotion labels are included in AFEW, *i.e.* anger, disgust, fear, happiness, sadness, surprise, and neutral. AFEW contains videos collected from different movies and TV serials with spontaneous expressions, various head poses, occlusions, and illuminations. AFEW is divided into three splits: Train (738 videos), Val (352 videos), and Test (653 videos).

DFEW [16]: The DFEW is a large-scale unconstrained dynamic facial expression database, containing 16,372

video clips extracted from over 1,500 different movies. It contains 12,059 single-label video clips and also includes seven emotion labels, *i.e.* anger, disgust, fear, happiness, sadness, surprise, and neutral.

4.2 Snippet Extraction and Implementation Details

We first unified the video length to 105 frames via interpolation and clipping operation, and detected face regions of each frame to the size of 224×224 via the Retinaface [7]. Then, we randomly selected one of the first 30 frames as the starting frame, and extracted the following 75 consecutive frames to form a video. Next, we split the 75 frames into 7 sub-videos, each of which had 15 frames, with five frames overlapping between each sub-video. To enhance expression movement variation, 5 frames were randomly sampled from each sub-video to form a new sub-video which is an expression snippet. Thus, $n = 7$ and $j = 5$. For training, the seven snippets were shuffled in a random order (the frame order within each snippet remained unchanged). For test, we only used the normal snippet order as input for robust FER.

We used the Pytorch for implementing the EST. The key training parameters include initial learning rate (0.0001), cosine annealing schedule to adjust the learning rate, mini-batch size (8), and warm up. The experiments were conducted on a PC with Intel(R) Xeon(R) Gold 6240C CPU at 2.60GHz and 128GB memory, and NVIDIA GeForce RTX 3090. Following the setting of other compared methods, we conducted a 10-fold person-independent validation on the BU-3DFE and MMI, a Train/Val set validation on the AFEW, and a 5-fold validation on DFEW dataset. We will release our source code to Github after acceptance.

4.3 Experiments on the BU-3DFE Dataset

Fig. 4(a) shows the confusion matrix of BU-3DFE for video FER by using our method. Among the six expressions, the highest accuracy are 95.0% of Happiness and Surprise, while the lowest accuracy is 80.0% for Fear, which has the least amount of facial expression movement and is difficult to distinguish with Disgust. The average FER accuracy is 88.17%.

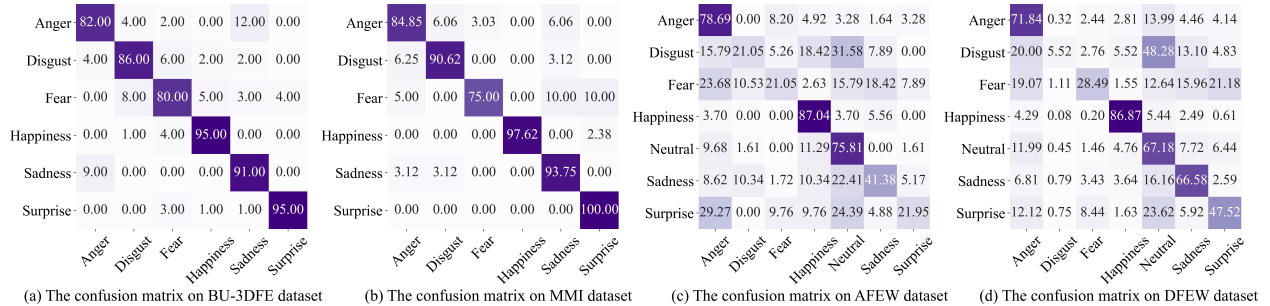


Figure 4: The confusion matrixes for video-based FER on the four datasets.

The average FER accuracy of the EST was compared with the state-of-the-art methods, including DeRL [46], FAN [32], ICNP [54], C3D [40], 2D+3D model [30], FERAtt+Rep+Cls [31] and C3D-LSTM [35] in Table 1. Compared to the best sequence-based result, the proposed EST improved the accuracy over 4.97%. This reveals that our method can effectively discover the more beneficial emotion-related cues by modeling the long-range emotion movement relation in videos.

Methods	Feature setting	Accuracy(%)
FAN [32]	frame-based	84.17
2D+3D model [30]	frame-based	87.66
FERAtt+Rep+Cls [31]	frame-based	82.11
DeRL [46]	peak frame-based	84.17
C3D [40]	sequence-based	82.18
ICNP [54]	sequence-based	83.20
C3D-LSTM [35]	sequence-based	79.17
Our EST	snippet-based	88.17

Table 1: Comparison results on the BU-3DFE dataset. Note: the best result is highlighted in bold.

4.4 Experiments on the MMI Dataset

Fig. 4(b) depicts the confusion matrix of MMI for video FER by using our method. We achieved 100% accuracy in Surprise category. The average accuracy of FER is 92.5%.

In comparison with the state-of-the-art video-based FER methods, Table 2 lists the average accuracy on the MMI dataset using deep learning-based methods with spatial feature representation (*i.e.*, AUDN [27], DeRL [46], LSTM [18], Deep generative-contrastive networks (DGCN) [19], Ensemble Network [37], SAANet [26], WMCNN-LSTM [50], WMDCNN [50]),

hand-crafted feature based methods (*i.e.*, collaborative expression representation (CER) extracted from the apex frames and LPQ-TOP [15] extracted from the whole sequence), and our EST. As shown in the table, the proposed EST outperformed existing state-of-the-art FER methods. Compared to the second best method, Ensemble Network [37], the EST improved the accuracy of 1.04%.

Methods	Feature setting	Accuracy(%)
DeRL [46]	frame-based	73.23
WMDCNN [50]	frame-based	78.20
AUDN [27]	peak frame-based	75.85
CER [23]	peak frame-based	70.12
Ensemble Network [37]	peak+neutral frame	91.46
LSTM [18]	sequence-based	78.61
DGCN [19]	sequence-based	81.53
LPQ-TOP+SRC [15]	sequence-based	64.11
SAANet [26]	sequence-based	87.06
WMCNN-LSTM [50]	sequence-based	87.10
Our EST	snippet-based	92.50

Table 2: Comparison results on the MMI dataset. Note: the best result is highlighted in bold.

4.5 Experiments on the AFEW Dataset

Fig. 4(c) shows the confusion matrix of FER on the challenging AFEW dataset. The average accuracy of FER achieved 54.26%. The highest accuracy is 87.04% of Happiness followed by Anger and Neutral, which respectively reach 78.69% and 75.81%. Although accuracies of Disgust and Fear are relatively lower than the other categories, our method still out-performs other methods in recognizing both emotions. This may be caused by better modeling the relations of subtle expression movements between snippets. Table 3 reports the accuracies using the

EST and state-of-the-art methods. It demonstrates that our method achieves the best performance with great robustness, meanwhile, has obvious advantages over other algorithms on the in-the-wild expression dataset.

Methods	Feature setting	Accuracy(%)
FAN [32]	frame-based	51.18
HoloNet [47]	frame-based	44.57
DSN-HoloNet [13]	frame-based	46.47
DSN-VGGFace [11]	frame-based	48.04
C3D [40]	sequence-based	30.11
DenseNet-161 [25]	sequence-based	51.44
VGG16+TP+SA [1]	sequence-based	49.00
Emotion-BEEU [21]	sequence-based	52.49
Mode variational LSTM [2]	sequence-based	51.44
Former-DFER [53]	sequence-based	50.92
Our EST	snippet-based	54.26

Table 3: Comparison results on AFEW 8.0 dataset. Note: the highest result is highlighted in bold.

4.6 Experiments on the DFEW Dataset

Fig. 4(d) shows the confusion matrix of FER on the large-scale DFEW dataset. The average accuracy of FER achieved 65.85% by using our method. The highest accuracy is 86.87% of Happiness followed by Anger, which achieves 71.84%. Although we only achieved 5.52% accuracy in the Disgust category due to the huge imbalance of categories in the DFEW (only occupies 1.22% in the DFEW dataset), the compared results in Table 4 shows that our method is still far superior to other algorithms. More detailed comparison results can be shown in Table 4. Compared to the state-of-the-art methods reported in [16], the FER accuracy of our EST achieved significant improvement (over 9.34%).

Methods	Feature setting	Accuracy(%)
3D ResNet-18,EC-STFL [16]	sequence-based	56.51
C3D,EC-STFL [16]	sequence-based	55.50
P3D,EC-STFL [16]	sequence-based	56.48
R3D18,EC-STFL [16]	sequence-based	56.19
VGG11+LSTM,EC-STFL [16]	sequence-based	56.25
Our EST	snippet-based	65.85

Table 4: Comparison results on DFEW dataset.

Transformer	AA-SFE	SSOP	Params(M)	MACs(G)	Acc(%)
✓			34.37	63.85	85.60
✓	✓		34.37	63.88	87.12
✓	✓	✓	42.78	63.89	88.17

Table 5: Ablation study of the proposed EST. Impact of integrating our different components (AA-SFE and SSOP) into the baseline Transformer on the BU-3DFE dataset.

Different attention	Params(M)	Acc(%)
w/o attention	34.37	85.60
self-attention	42.78	87.63
SE-like attention [12]	43.30	87.46
Our hierarchical attention	42.78	88.17

Table 6: Ablation study of different attention selection in AA-SFE. The best results are highlighted in bold.

4.7 Ablation experiment and analysis

To better understand the role of each module in the proposed EST, Table 5 presents the ablation results of the gradual addition AA-SFE and SSOP components to the baseline Transformer framework. The Transformer achieved a video-based FER accuracy of 85.60% on the BU-3DFE dataset. The further integration of AA-SFE improved the accuracy to 87.12%, as the AA-SFE aids in the extraction of snippet-level features via jointly hierarchical attentions. Thanks to learning the order sensitive representation, the addition of SSOP resulted in an increase of 1.05%.

Furthermore, Table 6 lists the recognition results with different attention selection in the AA-SFE. Obviously, two-level hierarchical attention used in AA-SFE achieved the best performance without any computational cost, helping to describe more informative snippet features.

In addition, Fig. 5 shows more analysis about the effect of the SSOP in the EST. In particular, Fig. 5(a) presents the distribution of the index of the snippet with the highest attention weight in EST with and without SSOP, respectively. Without SSOP (see the dark-blue column in Fig. 5(a)), we can observe that the EST always focused on the 3-rd snippet, which usually contains the peak changes in each test video. Alternatively, the SSOP can make EST distribute similar attention to all the snippets. We further illustrate the encoded emotion representation in 2D space using t-SNE visualization with and without using

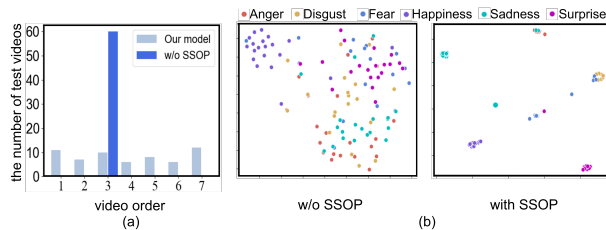


Figure 5: The effects of SSOP. (a) Comparison of index distributions of the snippet with the highest attention weight with and without SSOP in EST; (b) Comparison of t-SNE analysis with and without SSOP.

Methods	Input	Backbone	Params(M)	MACs(G)	fps	Acc
C3D-LSTM [35]	Video	ResNet-18	110.24	282.26	708	29.83
FERAtt [31]	Frame	ResNet-18	67.08	13.56	75	37.22
Dense161 [25]	Video	DenseNet-161	26.52	272.47	47	51.44
VGG16TPSA [1]	Video	VGG16	14.72	537.61	552	49.00
Our EST	Video	ResNet-18	42.78	63.89	412	54.26

Table 7: Comparison of model complexity and efficiency.

SSOP in Fig. 5(b). The results show that the SSOP helps obtain more discriminative representation by comprehensively making the Transformer model inter-snippet visual changes.

Model complexity Table 7 reports model parameters and computational costs of three spatial-temporal learning methods on the AFEW dataset. In general, our EST has the best performance (accuracy of 54.26%) with a small computational cost (63.89G MACs) and real-time speed (412 fps), which means that the proposed method exhibits improved accuracy and efficiency. More ablation studies and discussions can be seen in the supplementary material.

5 Conclusions and Future Works

In this paper, a novel expression snippet Transformer (EST) is proposed to better model elusive facial expression cues for robust facial expression recognition in untrimmed videos. The EST consists of four major components, *i.e.*, snippet decomposition, snippet-based feature extractor, the encoder-decoder based Transformer, the shuffled order prediction head. Due to effectively and efficiently modeling long-range expression spatial-temporal relations and subtle intra-/inter- snippet visual changes, the proposed method achieved highly improved performance and strong robustness for video-

based FER; the highest accuracies respectively reached 88.17%, 92.5%, 54.26%, and 65.85% on four challenging datasets (BU-3DFE, MMI, AFEW, and DFEW). In the future, we will introduce self-supervised learning to Transformer to model the extraction of emotion-rich features from complex unlabelled videos.

References

- [1] Masih Aminbeidokhti, Marco Pedersoli, Patrick Cardinal, and Eric Granger. Emotion recognition with spatial attention and temporal softmax pooling. In *International Conference on Image Analysis and Recognition*, pages 323–331. Springer, 2019.
- [2] Wissam J Baddar and Yong Man Ro. Mode variational lstm robust to unseen modes of variation: Application to facial expression recognition. In *Proceedings of the AAAI Conference on Artificial Intelligence*, volume 33, pages 3215–3223, 2019.
- [3] Sarah Adel Bargal, Emad Barsoum, Cristian Canton Ferrer, and Cha Zhang. Emotion recognition in the wild from videos using images. In *Proceedings of the 18th ACM International Conference on Multimodal Interaction (ICMI)*, pages 433–436, 2016.
- [4] Nicolas Carion, Francisco Massa, Gabriel Synnaeve, Nicolas Usunier, Alexander Kirillov, and Sergey Zagoruyko. End-to-end object detection with transformers. In *Proceedings of the European Conference on Computer Vision (ECCV)*, pages 213–229. Springer, 2020.
- [5] Yangyu Chen, Shuhui Wang, Weigang Zhang, and Qingming Huang. Less is more: Picking informative frames for video captioning. In *Proceedings of the European Conference on Computer Vision (ECCV)*, pages 358–373, 2018.
- [6] Zhigang Dai, Bolun Cai, Yugeng Lin, and Junying Chen. Up-detr: Unsupervised pre-training for object detection with transformers. In *Proceedings of the IEEE/CVF Conference on Computer Vision and Pattern Recognition*, pages 1601–1610, 2021.
- [7] Jiankang Deng, Jia Guo, Evangelos Ververas, Irene Kotzia, and Stefanos Zafeiriou. Retinaface: Single-shot multi-level face localisation in the wild. In *Proceedings of the IEEE Conference on Computer Vision and Pattern Recognition (CVPR)*, pages 5203–5212, 2020.
- [8] Jacob Devlin, Ming-Wei Chang, Kenton Lee, and Kristina Toutanova. BERT: Pre-training of deep bidirectional transformers for language understanding. In *Proceedings of the*

- 2019 Conference of the North American Chapter of the Association for Computational Linguistics: Human Language Technologies, Volume 1 (Long and Short Papers), pages 4171–4186, 2019.
- [9] Abhinav Dhall, OV Ramana Murthy, Roland Goecke, Jyoti Joshi, and Tom Gedeon. Video and image based emotion recognition challenges in the wild: Emotiw 2015. In *Proceedings of the 2015 ACM on International Conference on Multimodal Interaction (ICMI)*, pages 423–426, 2015.
- [10] Yin Fan, Xiangju Lu, Dian Li, and Yuanliu Liu. Video-based emotion recognition using cnn-rnn and c3d hybrid networks. In *Proceedings of the 18th ACM International Conference on Multimodal Interaction (ICMI)*, pages 445–450, 2016.
- [11] Yingruo Fan, Jacqueline CK Lam, and Victor OK Li. Video-based emotion recognition using deeply-supervised neural networks. In *Proceedings of the 20th ACM International Conference on Multimodal Interaction (ICMI)*, pages 584–588, 2018.
- [12] Jie Hu, Li Shen, and Gang Sun. Squeeze-and-excitation networks. In *Proceedings of the IEEE Conference on Computer Vision and Pattern Recognition (CVPR)*, pages 7132–7141, 2018.
- [13] Ping Hu, Dongqi Cai, Shandong Wang, Anbang Yao, and Yurong Chen. Learning supervised scoring ensemble for emotion recognition in the wild. In *Proceedings of the 19th ACM International Conference on Multimodal Interaction (ICMI)*, pages 553–560, 2017.
- [14] M. W. Huang, Z. W. Wang, and Z. L. Ying. A new method for facial expression recognition based on sparse representation plus lbp. In *2010 3rd International Congress on Image and Signal Processing (CISP)*, volume 4, pages 1750–1754. IEEE, 2010.
- [15] Bihan Jiang, Michel Valstar, Brais Martinez, and Maja Pantic. A dynamic appearance descriptor approach to facial actions temporal modeling. *IEEE transactions on cybernetics*, 44(2):161–174, 2013.
- [16] Xingxun Jiang, Yuan Zong, Wenming Zheng, Chuangao Tang, Wanchuang Xia, Cheng Lu, and Jiateng Liu. Dfew: A large-scale database for recognizing dynamic facial expressions in the wild. In *Proceedings of the 28th ACM International Conference on Multimedia (MM)*, pages 2881–2889, 2020.
- [17] Heechul Jung, Sihaeng Lee, Junho Yim, Sunjeong Park, and Junmo Kim. Joint fine-tuning in deep neural networks for facial expression recognition. In *Proceedings of the IEEE International Conference on Computer Vision (ICCV)*, pages 2983–2991, 2015.
- [18] Dae Hoe Kim, Wissam J Baddar, Jinhyeok Jang, and Yong Man Ro. Multi-objective based spatio-temporal feature representation learning robust to expression intensity variations for facial expression recognition. *IEEE Transactions on Affective Computing*, 10(2):223–236, 2017.
- [19] Youngsung Kim, ByungIn Yoo, Youngjun Kwak, Changkyu Choi, and Junmo Kim. Deep generative-contrastive networks for facial expression recognition. *arXiv preprint arXiv:1703.07140*, 2017.
- [20] Boris Knyazev, Roman Shvetsov, Natalia Efremova, and Artem Kuharenko. Convolutional neural networks pre-trained on large face recognition datasets for emotion classification from video. *arXiv preprint arXiv:1711.04598*, 2017.
- [21] Vikas Kumar, Shivansh Rao, and Li Yu. Noisy student training using body language dataset improves facial expression recognition. In *Proceedings of the European Conference on Computer Vision (ECCV)*, pages 756–773. Springer, 2020.
- [22] Jiyoung Lee, Seungryong Kim, Sunok Kim, Jungin Park, and Kwanghoon Sohn. Context-aware emotion recognition networks. In *Proceedings of the IEEE International Conference on Computer Vision (ICCV)*, pages 10143–10152, 2019.
- [23] Seung Ho Lee, Wissam J Baddar, and Yong Man Ro. Collaborative expression representation using peak expression and intra class variation face images for practical subject-independent emotion recognition in videos. *Pattern Recognition*, 54:52–67, 2016.
- [24] Shan Li and Weihong Deng. Deep facial expression recognition: A survey. *IEEE Transactions on Affective Computing*, PP(99), 2020.
- [25] Chuanhe Liu, Tianhao Tang, Kui Lv, and Minghao Wang. Multi-feature based emotion recognition for video clips. In *Proceedings of the 20th ACM International Conference on Multimodal Interaction (ICMI)*, pages 630–634, 2018.
- [26] Daizong Liu, Xi Ouyang, Shuangjie Xu, Pan Zhou, Kun He, and Shiping Wen. Saanet: Siamese action-units attention network for improving dynamic facial expression recognition. *Neurocomputing*, 413:145–157, 2020.
- [27] Mengyi Liu, Shaoxin Li, Shiguang Shan, and Xilin Chen. Au-inspired deep networks for facial expression feature learning. *Neurocomputing*, 159:126–136, 2015.
- [28] Christoph Lüscher, Eugen Beck, Kazuki Irie, Markus Kitzka, Wilfried Michel, Albert Zeyer, Ralf Schlüter, and Hermann Ney. Rwth asr systems for librispeech: Hybrid vs attention. In *Interspeech*, pages 231–235, 2019.

- [29] Patrick Lucey, Jeffrey F Cohn, Takeo Kanade, Jason Saragih, Zara Ambadar, and Iain Matthews. The extended cohn-kanade dataset (ck+): A complete dataset for action unit and emotion-specified expression. In *2010 IEEE Computer Society Conference on Computer Vision and Pattern Recognition Workshops (CVPRW)*, pages 94–101, 2010.
- [30] Thai Son Ly, Nhu-Tai Do, Soo-Hyung Kim, Hyung-Jeong Yang, and Guee-Sang Lee. A novel 2d and 3d multimodal approach for in-the-wild facial expression recognition. *Image and Vision Computing*, 92:103817, 2019.
- [31] Pedro D Marrero Fernandez, Fidel A Guerrero Pena, Tsang Ren, and Alexandre Cunha. Feratt: Facial expression recognition with attention net. In *Proceedings of the IEEE Conference on Computer Vision and Pattern Recognition Workshops (CVPRW)*, pages 837–846, 2019.
- [32] Debin Meng, Xiaojiang Peng, Kai Wang, and Yu Qiao. Frame attention networks for facial expression recognition in videos. In *2019 IEEE International Conference on Image Processing (ICIP)*, pages 3866–3870. IEEE, 2019.
- [33] Daniel Neimark, Omri Bar, Maya Zohar, and Dotan Asselemani. Video transformer network. *arXiv preprint arXiv:2102.00719*, 2021.
- [34] Niki Parmar, Ashish Vaswani, Jakob Uszkoreit, Lukasz Kaiser, Noam Shazeer, Alexander Ku, and Dustin Tran. Image transformer. In *International Conference on Machine Learning (ICML)*, pages 4055–4064. PMLR, 2018.
- [35] Paritosh Parmar and Brendan Tran Morris. Learning to score olympic events. In *Proceedings of the IEEE Conference on Computer Vision and Pattern Recognition Workshops (CVPRW)*, pages 20–28, 2017.
- [36] Alec Radford, Jeffrey Wu, Rewon Child, David Luan, Dario Amodei, and Ilya Sutskever. Language models are unsupervised multitask learners. *OpenAI blog*, 1(8):9, 2019.
- [37] Ning Sun, Qi Li, Ruizhi Huan, Jixin Liu, and Guang Han. Deep spatial-temporal feature fusion for facial expression recognition in static images. *Pattern Recognition Letters*, 119:49–61, 2019.
- [38] Gabriel Synnaeve, Qiantong Xu, Jacob Kahn, Tatiana Likhomanenko, Edouard Grave, Vineel Pratap, Anuroop Sriram, Vitaliy Liptchinsky, and Ronan Collobert. End-to-end asr: from supervised to semi-supervised learning with modern architectures. *arXiv preprint arXiv:1911.08460*, 2019.
- [39] Ashish Tawari and Mohan Manubhai Trivedi. Face expression recognition by cross modal data association. *IEEE Transactions on Multimedia*, 15(7):1543–1552, 2013.
- [40] Du Tran, Lubomir Bourdev, Rob Fergus, Lorenzo Torresani, and Manohar Paluri. Learning spatiotemporal features with 3d convolutional networks. In *Proceedings of the IEEE international conference on computer vision (ICCV)*, pages 4489–4497, 2015.
- [41] Michel Valstar and Maja Pantic. Induced disgust, happiness and surprise: an addition to the mmi facial expression database. In *Proc. 3rd Intern. Workshop on EMOTION (satellite of LREC): Corpora for Research on Emotion and Affect*, page 65. Paris, France., 2010.
- [42] Ashish Vaswani, Noam Shazeer, Niki Parmar, Jakob Uszkoreit, Llion Jones, Aidan N. Gomez, undefinedukasz Kaiser, and Illia Polosukhin. Attention is all you need. In *Proceedings of the 31st International Conference on Neural Information Processing Systems (NeurIPS)*, page 6000–6010. Curran Associates Inc., 2017.
- [43] Valentin Vielzeuf, Stéphane Pateux, and Frédéric Jurie. Temporal multimodal fusion for video emotion classification in the wild. In *Proceedings of the 19th ACM International Conference on Multimodal Interaction (ICMI)*, pages 569–576, 2017.
- [44] Zhen Wang and Zilu Ying. Facial expression recognition based on local phase quantization and sparse representation. In *2012 8th International Conference on Natural Computation*, pages 222–225. IEEE, 2012.
- [45] Jianlong Wu, Zhouchen Lin, Wenming Zheng, and Hongbin Zha. Locality-constrained linear coding based bi-layer model for multi-view facial expression recognition. *Neurocomputing*, 239:143–152, 2017.
- [46] Huiyuan Yang, Umur Ciftci, and Lijun Yin. Facial expression recognition by de-expression residue learning. In *Proceedings of the IEEE Conference on Computer Vision and Pattern Recognition (CVPR)*, pages 2168–2177, 2018.
- [47] Anbang Yao, Dongqi Cai, Ping Hu, Shandong Wang, Liang Sha, and Yurong Chen. Holonet: towards robust emotion recognition in the wild. In *Proceedings of the 18th ACM International Conference on Multimodal Interaction (ICMI)*, pages 472–478, 2016.
- [48] Lijun Yin, Xiaozhou Wei, Yi Sun, Jun Wang, and Matthew J Rosato. A 3d facial expression database for facial behavior research. In *7th International Conference on Automatic Face and Gesture Recognition (FGR)*, pages 211–216. IEEE, 2006.
- [49] Zhenbo Yu, Qinshan Liu, and Guangcan Liu. Deeper cascaded peak-piloted network for weak expression recognition. *The Visual Computer*, 34(12):1691–1699, 2018.

- [50] Hepeng Zhang, Bin Huang, and Guohui Tian. Facial expression recognition based on deep convolution long short-term memory networks of double-channel weighted mixture. *Pattern Recognition Letters*, 131:128–134, 2020.
- [51] Tong Zhang, Wenming Zheng, Zhen Cui, Yuan Zong, Jingwei Yan, and Keyu Yan. A deep neural network-driven feature learning method for multi-view facial expression recognition. *IEEE Transactions on Multimedia*, 18(12):2528–2536, 2016.
- [52] Xiangyun Zhao, Xiaodan Liang, Luoqi Liu, Teng Li, Yugang Han, Nuno Vasconcelos, and Shuicheng Yan. Peak-piloted deep network for facial expression recognition. In *Proceedings of the European Conference on Computer Vision (ECCV)*, pages 425–442. Springer, 2016.
- [53] Zengqun Zhao and Qingshan Liu. Former-dfer: Dynamic facial expression recognition transformer. In *Proceedings of the ACM International Conference on Multimedia*, 2021.
- [54] Qingkai Zhen, Di Huang, Yunhong Wang, and Liming Chen. Muscular movement model-based automatic 3d/4d facial expression recognition. *IEEE Transactions on Multimedia*, 18(7):1438–1450, 2016.

Supplementary Material for “Expression Snippet Transformer for Robust Video-based Facial Expression Recognition”

Yuanyuan Liu¹, Wenbin Wang¹, Chuanxu Feng¹, Haoyu Zhang¹, Zhe Chen^{*2}, and Yibing Zhan³

¹China University of Geosciences (Wuhan)

¹{liuyy, wangwenbin, fcxfcx, zhanghaoyu}@cug.edu.cn

²The University of Sydney

²zhe.chen1@sydney.edu.au

³Jingdong

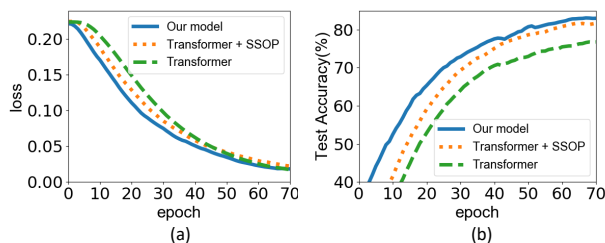
³zhanyibing@jd.com

September 20, 2021

The content of our supplementary material is organized as follows.

1. The training loss and testing accuracy of the EST with different components.
2. Effect of important parameters in our framework.
3. Compare with different backbones in our framework.
4. Visualization of different video expression representations.
5. Visualization of attention weights modelled by our EST and the Transformer.
6. Detailed description of the Transformer architecture used in our EST.

belong to the baseline Transformer. From the view of the decline rates of training losses, obviously, the gradual addition of AA-SFE and SSOP improved the Transformer performance on both training speed and stability. Meanwhile, the proposed EST with AA-SFE and SSOP is easier to achieve higher accuracy on the test set.



1 Training Loss and Testing Accuracy Curves for different component study

Fig. 1 shows the training and prediction procedures of the EST with different components. The green dotted curves

Figure 1: The learning procedure for the EST with different components during training and testing. (a) The training loss variation in terms of epochs, (b) the testing accuracy variation in terms of epochs.

*Corresponding author

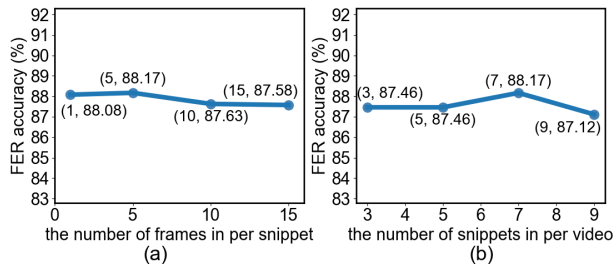


Figure 2: The impact of the number of frames in per snippet and the number of snippets in per video for FER on the BU-3DFE dataset. (a) The effect of the number of frames in per snippet, (b) the effect of the number of expression snippets in per video.

2 Effect of Important Parameters

In Fig. 2, we present the FER accuracy curves on the BU-3DFE dataset, which effected by the number of frames in per snippet and the number of snippets in per video. As shown in the Fig. 2 (a), the accuracy achieved to the highest 88.17% when we set the number of frames of each snippet to 5. Fig. 2 (b) shows that the accuracy reached the highest when the number of snippets in per video is set to 7. Besides, we also observe that different snippet amounts and snippet lengths only resulted in minor performance changes, suggesting that these hyperparameters are less important to our method. Hence, thanks to the long-range relation modeling ability of the Transformer, our EST can be easily extended to adapt to videos of almost any length upon proper training.

To evaluate the effect of the types of shuffle order in SSOP learning, Fig.3 presents the variation curves of FER accuracy and snippet order prediction accuracy according to the number of shuffle order types on the BU-3DFE dataset. As shown in Fig.3 (a)(b), when the number of the types is 10, both the FER accuracy and snippet order prediction accuracy reach the highest 88.17% and 55.43%, respectively. Therefore, during the training, we set the types of shuffle order to 10.

Additionally, Fig.4 presents the calculation results of cosine similarity in the AA-SFE. Due to small movement variation between expression snippets, all of the calculated cosine similarities are above 0.4, avoiding the oc-

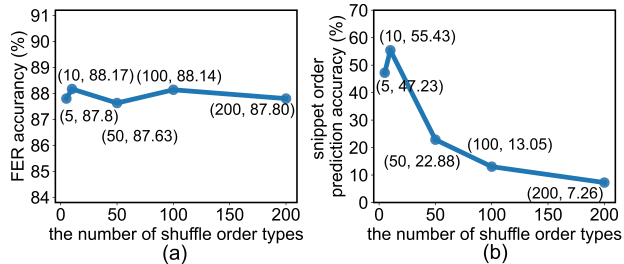


Figure 3: The influence of the types of shuffle order for FER accuracy and order prediction accuracy on the BU-3DFE dataset. (a) FER accuracy, (b) snippet order prediction accuracy.

currence of negative operation in the feature summation. And we set a small value $1e - 8$ to avoid division by zero.

3 Comparison of Different Backbones

Backbone	Params(M)	MACs(G)	Acc(%)
ResNet-18[1]	42.78	63.89	54.26
ResNet-34[1]	52.88	128.54	51.99
ResNet-50[1]	272.49	144.06	53.12

Table 1: Comparison of different backbones.

Table. 1 reports model parameters, computational cost, and FER accuracies of three different backbones in processing the AFEW dataset. Obviously, as the backbone network deepens, the proposed model requires more parameters and computational cost. However, the deeper models did not bring a significant increase in FER accuracy. On the contrary, the smaller ResNet-18 as the backbone resulted in the best performance (the FER accuracy of 54.26%).

4 Visualization Results of Expression Representations

In Fig. 5, we visualized the emotion features with different settings in a 2D feature space by using the t-SNE [2]

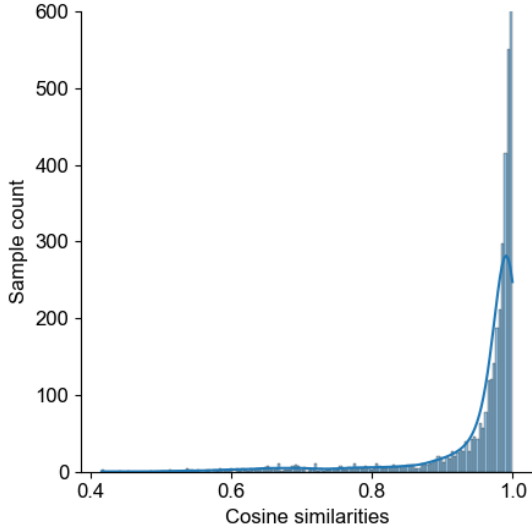


Figure 4: The distribution of cosine similarity

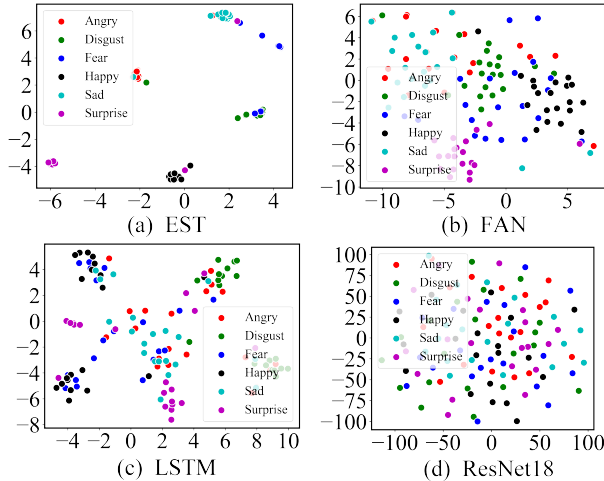


Figure 5: The comparison of different representations in 2D space by t-SNE visualization. (a) The unified salient emotion representation learned by EST, (b) the frame-based features learned by FAN [3], (c) the sequence-based features learned by LSTM, (d) the frame-based features learned by ResNet-18.

on the BU-3DFE dataset. Compared the other emotion features, we can observe that the comprehensive and robust expression representation learned by the EST includes more visual change cues and can significantly be separated according to different expression categories.

5 Visualization Results of Attention Weights

Fig. 6 shows the comparison of expression relation curves for modeling subtle facial expression movements between the vanilla Transformer and the proposed EST on four videos from the BU-3DFE, MMI, AFEW, DFEW dataset, respectively. From the Fig. 6(a), the vanilla Transformer tends to focus on the frames with peak expression patterns, which are easily affected by noises such as head pose and other non-expression changes. On the contrary, by decomposing videos into snippets, although the changes of expression movements of intra-/inter-snippets are very subtle in a video, our EST focuses on all expression snippet changes and improves modeling of intra-snippet and inter-snippet subtle facial expression changes, meanwhile, effectively locates the most informative expression snippet by the modelled expression attention weights (see the values of the Ordinate in Fig. 6(b)). It is evident that the EST succeeded at focusing on comprehensive expression movements according to the relations of snippet features to the *emotion query embedding* and achieved more robust FER.

6 Detailed Transformer architecture

The detailed description of the transformer used in EST, is given in Fig. 7. Snippet features \mathcal{R} from the AA-SFE extractors are first passed through the transformer encoder, together with positional encoding. Then the decoder receives the emotion query embedding (initially from $\mathcal{N}(0, 1)$) and the encoded snippet features H , and produces the emotion representation T through three decoder layers.

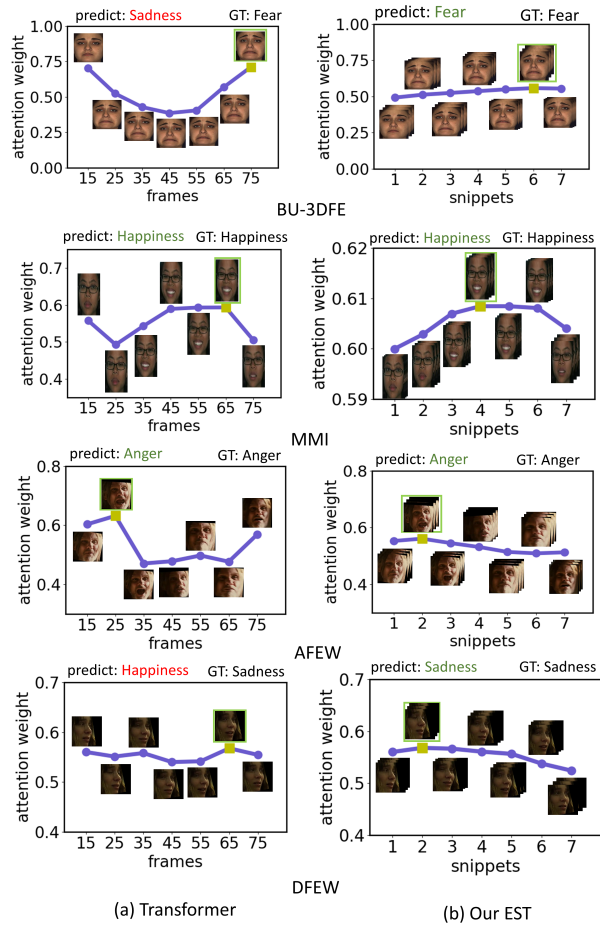


Figure 6: Comparison of modeling subtle facial expression movements in FER on the BU-3DFE, MMI, AFEW, DFEW dataset. (a) vanilla Transformer, (b) our EST. Note: the green square is located at the position of the most informative expression snippet with the most attention weight.

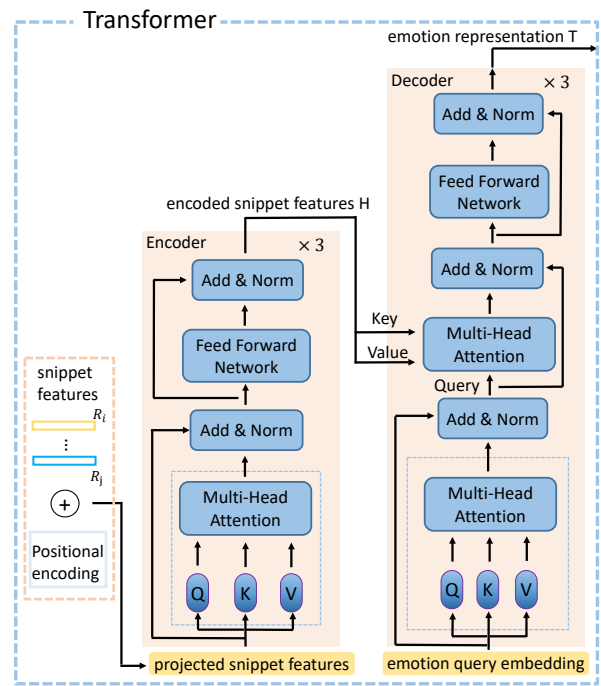


Figure 7: Architecture of the transformer used in EST.

References

- [1] Kaiming He, Xiangyu Zhang, Shaoqing Ren, and Jian Sun. Deep residual learning for image recognition. In *Proceedings of the IEEE Conference on Computer Vision and Pattern Recognition (CVPR)*, pages 770–778, 2016.
- [2] Laurens van der Maaten and Geoffrey Hinton. Visualizing data using t-sne. *Journal of machine learning research*, 9(Nov):2579–2605, 2008.
- [3] Debin Meng, Xiaojiang Peng, Kai Wang, and Yu Qiao. Frame attention networks for facial expression recognition in videos. In *2019 IEEE International Conference on Image Processing (ICIP)*, pages 3866–3870. IEEE, 2019.